Journal of Alloys and Compounds 509 (2011) 221–225

Contents lists available at ScienceDirect

Journal of Alloys and Compounds

journal homepage: www.elsevier.com/locate/jallcom

Synthesis, crystal and band structures, and optical properties of a new framework mercury pnictides: $[Hg_4As_2](InBr_{3.5}As_{0.5})$ with tridymite topology

Jian-Ping Zou[a,b,*], Sheng-Lian Luo[c], Xing-Hua Tang[c], Ming-Jun Li[c], Ai-Qin Zhang[c], Qiang Peng[c,**], Guo-Cong Guo[b]

[a] Key Laboratory of Nondestructive Testing (Nanchang Hangkong University), Ministry of Education, 696 Fenghe South Road, Nanchang, Jiangxi 330063, PR China
[b] State Key Laboratory of Structural Chemistry, Fujian Institute of Research on the Structure of Matter, Chinese Academy of Sciences, Fuzhou, Fujian 350002, PR China
[c] School of Environmental and Chemical Engineering, Nanchang Hangkong University, Nanchang, Jiangxi 330063, PR China

ARTICLE INFO

Article history:
Received 15 June 2010
Received in revised form 22 August 2010
Accepted 6 September 2010
Available online 16 September 2010

Keywords:
Crystal structure
Open-frameworks
Optical properties
Tridymite topology
Solid state reactions

ABSTRACT

A new framework compound, $[Hg_4As_2](InBr_{3.5}As_{0.5})$ (**1**), has been prepared by the solid-state reaction of Hg_2Br_2 with elemental In and As at 450 °C. Compound **1** crystallizes in the space group P_{63}/mmc of the Hexagonal system with two formula units in a cell: $a = b = 7.7408(6)$ Å, $c = 12.5350(19)$ Å, $V = 650.47(12)$ Å^3. The crystal structure of **1** features a novel 3D framework, $[Hg_4As_2]^{2+}$ with tridymite topology. The optical properties were investigated in terms of the diffuse reflectance and infrared spectra. The electronic band structure along with density of states (DOS) calculated by DFT method indicates that the present compound is semiconductor, and the optical absorption is mainly originated from the charge transitions from Br-4p and As-4p states to Hg-6s and In-5p states.

1. Introduction

Microporous and open-framework inorganic solids have been extensively studied due to their industrial applications in catalysis, separation, and ion-exchange processes [1–5]. In the past decades, natural geological examples have been followed by transforming common silicate, aluminate, and phosphate building blocks into zeolite-type materials with microporous frameworks [6–10]. However, the known classes of microporous materials are overwhelmingly dominated by oxide, mixed oxide/fluoride matrices, sulfides, or halides [11–17]. Recently, mercury pnictides are well attractive because of their abundant structural features and distinctive electronic properties [18–23]. For instance, the propensity of mercury to linear two-coordination or to tetrahedral coordination can be exploited in the design of open-framework inorganic solids. Till now, two principal types of frameworks can be distinguished. The first type is the topology with the formula of $(Hg_6Z_4)^{4+}$ (Z = P, As, Sb) [24–28] possessing cavities of two different sizes in close proximity that are capable of trapping two different types of guests. The second type is the analogues of the well-known Millon's base salts [29–31], composed of cationic frameworks with the formula $[Hg_4Z_2]^{2+}$ (Z = P, As), which adopt a tridymite-like topology filled with different tetrahedral anions. Unlike the first type of topology, where there are more than 20 framework compounds have been synthesized, only four examples with the second type of topology, including $(Hg_2P)_2(HgBr_4)$ [32], $(Hg_2P)_2(ZnI_4)$ [33], $(Hg_2As)_2(ZnI_4)$ [34], and $(Hg_2As)_2(CdI_4)$ [35], have been reported in the literature. Further studies on inorganic framework compounds constructed from mercury pnictides are of fundamental importance.

Recently, we have begun a systematic investigation of mercury pnictide-based cationic frameworks to further explore new open-framework inorganic solids. Fortunately, our ongoing research in this field has resulted in some interesting framework compounds [21,27,28,35]. As a continuation of the previous work, in order to obtain new framework compounds based on the mercury pnictides, we selected indium atom as coordination center for the tetrahedral guests and changed the halogen atoms from Cl to I in the present work. Then we only succeeded in synthesizing a new quaternary phase, $[Hg_4As_2](InBr_{3.5}As_{0.5})$ (**1**), which is a new type of open-framework compounds with tridymite topology for mercury pnictides. Herein, we report the synthesis, crystal and band structures, as well as optical properties of the new framework compounds.

* Corresponding author at: Key Laboratory of Nondestructive Testing (Nanchang Hangkong University), Ministry of Education, 696 Fenghe South Road, Nanchang, Jiangxi 330063, PR China. Tel.: +86 791 3953377; fax: +86 791 3953373.
** Corresponding author.
E-mail addresses: zjp_112@126.com (J.-P. Zou), qiangpeng@tom.com (Q. Peng).

0925-8388/$ – see front matter © 2010 Elsevier B.V. All rights reserved.
doi:10.1016/j.jallcom.2010.09.035

2. Experimental and computational procedures

2.1. Materials and measurement

All of the chemicals were analytically pure (>99.99%) and used without further purification. The UV–vis spectrum of **1** was recorded at the room temperature on a computer-controlled PE Lambda 900 UV–vis spectrometer equipped with an integrating sphere in the wavelength range 200–2000 nm. A $BaSO_4$ plate was used as a reference, on which the finely ground powder of the sample was coated. The absorption spectrum was calculated from reflection spectrum by the Kubelka–Munk function [36,37]: $\alpha/S = (1-R)^2/2R$, where α is the absorption coefficient, S is the scattering coefficient that is practically wavelength independent when the particle size is larger than 5 μm, and R is the reflectance. The energy gap was determined as the intersection point between the energy axis at the absorption offset and the line extrapolated from the linear portion of the absorption edge in the α/S versus E (eV) plot. The IR spectrum was recorded by using a Nicolet Magana 750 FT-IR spectrophotometer in the range of 4000–400 cm^{-1}. A Powdery sample was pressed into pellets with KBr. The IR spectrum is given in Fig. S1.

2.2. Synthesis of $[Hg_4As_2](InBr_{3.5}As_{0.5})$ (**1**)

Single Crystals of **1** were prepared by the solid-state reaction of a mixture of Hg_2Br_2 (1 mmol, 561 mg), In (0.3 mmol, 35 mg), and As (0.5 mmol, 38 mg) at 320 °C. The starting materials were ground into fine powders in an agate mortar and pressed into a pellet, followed by being loaded into a Pyrex tube, evacuated to 1×10^{-4} Torr, and flame-sealed. The tube was placed into a computer-controlled furnace, heated from room temperature to 250 °C at a rate of 50 °C/h, kept at 250 °C for 4 h. The tube was then heated to 400 °C at 25 °C/h, kept at 400 °C for 120 h, and then slowly cooled down to 100 °C at a rate of 2 °C/h. Finally, it was cooled down to the room temperature over 10 h. A crop of dark red crystals of **1** that are stable in air were obtained. Semiquantitative microscope element analysis on several single crystals of **1** was performed on a field-emission scanning electron microscope (FESEM, JSM6700F) equipped with an energy dispersive X-ray spectroscope (EDS, Oxford INCA). The result confirms the presence of Hg, In, As and Br in the approximate molar ratio 7.9:2.1:5.1:6.9 and no other elements detected, which is in agreement with that by the X-ray diffraction analysis below.

2.3. X-ray crystallographic studies

A dark red single crystal of **1** was mounted on a glass fiber for the X-ray diffraction analysis. Data was collected on a Rigaku AFC7R diffractometer equipped with a graphite-monochromated Mo Kα radiation (λ = 0.71073 Å) at 293 K. Intensities were corrected for LP factors, and for empirical absorption using ψ scan technique. The structure was solved by direct methods and refined on F^2 with full-matrix least-squares techniques using Siemens SHELXTL version 5 package of crystallographic software [38]. The final refinements included anisotropic displacement parameters for all atoms and a secondary extinction correction. As for the disordered Br1 and As2 atoms, the occupancies of Br1 and As2 were firstly refined by setting the same coordinate and U_{eq} for them with the sum of site occupation at 1 (EXYZ Br1 As2; EADP Br1 As2; sump 1.0 0.01 1.0 2 1.0 3). Then the refined results show that the occupancies of Br1 and As2 are both approximate to 1/2. So the structure was lastly refined by fixing the occupancy of Br1 and As2 at 1/2 with setting the same coordinate and U_{eq} for them. As a result, the U_{eq} of Br1 and As2 atoms is comparable with those of Hg, In and other Br and As atoms. Therefore, the occupancies of 1/2 for both Br1 and As2 are reasonable. And they satisfy the requirement of balance of charge for the compound. As for the rather poor single crystal data (R_{int} = 0.1020 and R_1 = 0.0624), this maybe caused by the imperfect crystals or the diorder of guest anions. The crystallographic data of **1** is listed in Table 1. Selected bond lengths and bond angels are given in Table 2.

2.4. Computational descriptions

The crystallographic data of the present compound determined by X-ray single-crystal diffraction was used to calculate its electronic band structure. The calculation of electronic band structure along with the density of states (DOS) was performed with the CASTEP code [39] based on the density functional theory (DFT) using a plane-wave expansion of the wave functions and norm-conserving pseudopotential [40] in which the orbital electrons of Br-$4s^24p^5$, As-$4s^24p^3$, In-$5s^25p^1$, and Hg-$5d^{10}6s^2$ were treated as valence electrons. We used the generalized gradient approximation (GGA) in the scheme of Perdew–Burke–Eruzerhof (PBE) to describe the exchange and correlation potential, since the GGA was more widely used to calculate and analyze band structures of the inorganic compounds than the local-density approximation (LDA) [41–43]. To confirm the convergence of our calculations, we carefully investigated the dependences of the total energy on the cutoff energy and the k-point set mesh according to the Monkhorst–Pack grid. As shown in Fig. S2, when the k-point set mesh is fixed in 3 × 3 × 2, the change in total energy is less than 0.05 eV when the cutoff energy is higher than 450 eV; on the other hand, when the cutoff energy is fixed in 450 eV, the convergence in total energy is very well when the k-point set mesh is beyond 3 × 3 × 2. In consideration of computational cost, we choose the cutoff energy to be in 450 eV, and the Brillouin-zone sampling mesh parameters for the k-point set are 3 × 3 × 2.

Table 1
Crystal data and structure refinement parameters for **1**.

Empirical formula	$[Hg_4As_2](InBr_{3.5}As_{0.5})$
Formula mass [g/mol]	1384.17
Crystal color	Dark red
Crystal habit	Prism
Crystal system	Hexagonal
Space group	P_{63}/mmc
a [Å]	7.7408(6)
c [Å]	12.5350(19)
Volume [$Å^3$]	650.47(12)
Z	2
λ (Mo Kα) [Å]	0.71073
$D_{calcd.}$ [g/cm^3]	7.067
μ [mm^{-1}]	65.793
$F(0\,0\,0)$	1148
θ Range [°]	3.25–25.22
Reflections collected	868
Observed reflections	162
Independent reflections	257
R_{int}	0.1020
R_1,[a] wR_2[b]	0.0624, 0.1705
GOF	1.166
$\Delta\rho_{max}$ and $\Delta\rho_{min}$ [$e/Å^3$]	2.582, −2.391

[a] $R = \sum||F_o| - |F_c||/\sum|F_o|$.

[b] $R_w = \{\sum[w(F_o^2 - F_c^2)^2]/\sum[w(F_o^2)^2]\}^{1/2}$.

Table 2
Selected bond distances (Å) and bond angles (°) for **1**.[a]

Hg(1)–As(1) × 2	2.367(4)	In(1)–Br(2) × 3	2.470(4)
Hg(2)–As(1) × 2	2.353(12)	In(1)–Br(1)	2.479(7)
As(1)#1–Hg(1)–As(1)	180.0(5)	Hg(1)–As(1)–Hg(1)#5 × 3	109.7(3)
As(1)–Hg(2)–As(1)#2	180.000(1)	Hg(2)–As(1)–Hg(1) × 3	109.3(3)
Br(2)#3–In(1)–Br(2) × 3	113.25(13)	In(1)#4–Br(1)–In(1)	180.0
Br(2)–In(1)–Br(1) × 3	105.36(16)		

[a] Symmetry transformations used to generate equivalent atoms: #1 $-x+1, -y, -z$; #2 $x, y, -z+1/2$; #3 $-y, x-y, z$; #4 $-x, -y, -z$; #5 $-y+1, x-y, z$.

3. Results and discussion

As shown Fig. 1, the crystal structure of **1** possesses a novel 3D cationic framework of $AsHg_4$ tetrahedra with tridymite topology. Among the framework, the mercury atoms have linear coordina-

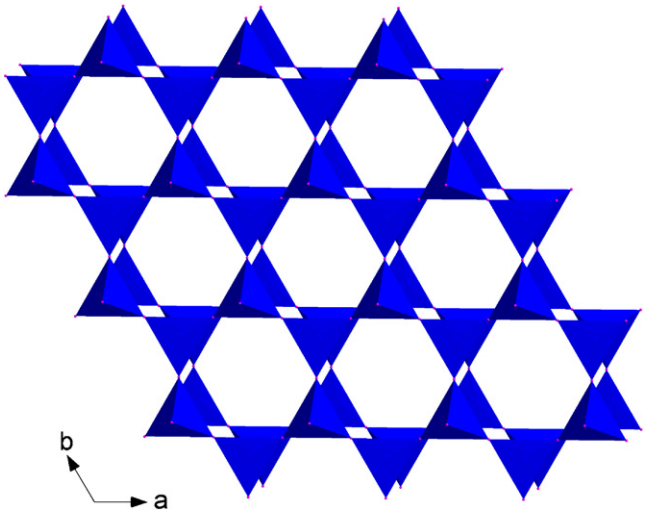

Fig. 1. The 3D open-framework with tridymite topology in **1** viewed along the c axis. Black tetrahedra represent $AsHg_4$ tetrahedra. (For interpretation of the references to color in this figure legend, the reader is referred to the web version of the article.)

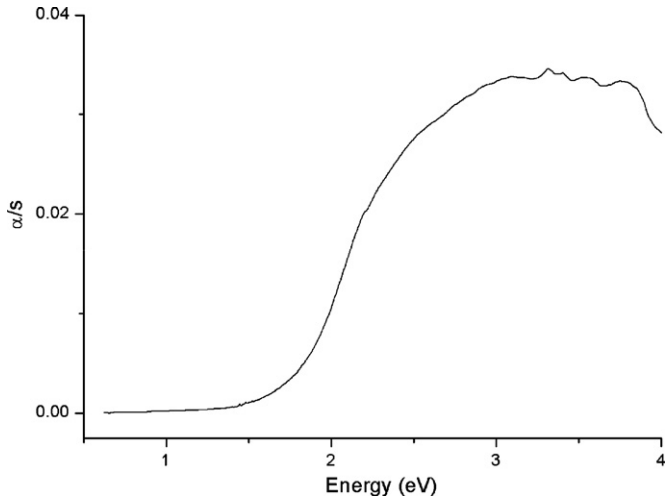

Fig. 2. Diffuse reflectance spectrum of **1**.

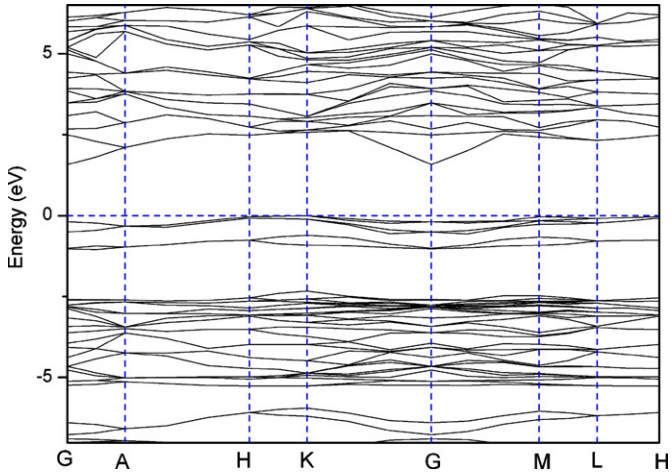

Fig. 3. The band structure of **1** (the Femi level is set at 0 eV, and the bands are shown only between −7 and 6 eV for clarity).

tion with the As–Hg–As bond angle of 180°, while the arsenic atoms possess an almost regular tetrahedral coordination by four mercury atoms with the Hg–As–Hg bond angle of 109.5° (Fig. S3 and Table 2). And these tetrahedra share corners each other through mercury atoms to form the 3D network with channels along the *c* direction (Fig. 1). Interestingly, unlike the present compound possing regular tetrahedra composed of mercury pnictides, distorted tetrahedra are formed by mercury pnictides among the reported compounds, such as $(Hg_2P)_2(HgBr_4)$ [32], $(Hg_2P)_2(ZnI_4)$ [33], $(Hg_2As)_2(ZnI_4)$ [34], as well as $(Hg_2As)_2(CdI_4)$ [35]. And this results in forming less ordered open-frameworks with lower symmetry among the four reported compounds (space group P_{63}/mmc for **1** but $P2_1$ for them). Therefore, unlike the above two kinds of open-frameworks composed of mercury pnictides reported in the literature [24–28,32–35], the open-framework composed of $AsHg_4$ tetrahedra in **1** is a new type of one with a novel tridymite topology. As for the guest anions, it can be regarded as a 1D corner-sharing Br_5 trigonal bipyramidal anionic network with 1/2 Br_5 polyhedra being occupied by In atoms (Fig. S4), which is embedded in the channels with the shortest Hg–Br bond distance being 3.81 Å.

There are two crystallographically independent mercury atoms in the structure of **1**. Analogues to the compound $(Hg_2As)_2(CdI_4)$ [35], the mercury atoms are all almost linearly coordinated by two arsenic atoms in **1**. The Hg–As bond distances range from 2.353(12) to 2.367(4) Å, which lie in the normal range of the Hg–As separations in mercury arsenidehalides [44,45] The In–Br bond distances range from 2.470(4) to 2.479(7) Å, which are shorter than those found in indium bromides [46–48]

In **1**, the distances between the bromine atoms of the guest anions and the mercury atoms in the host open-framework range

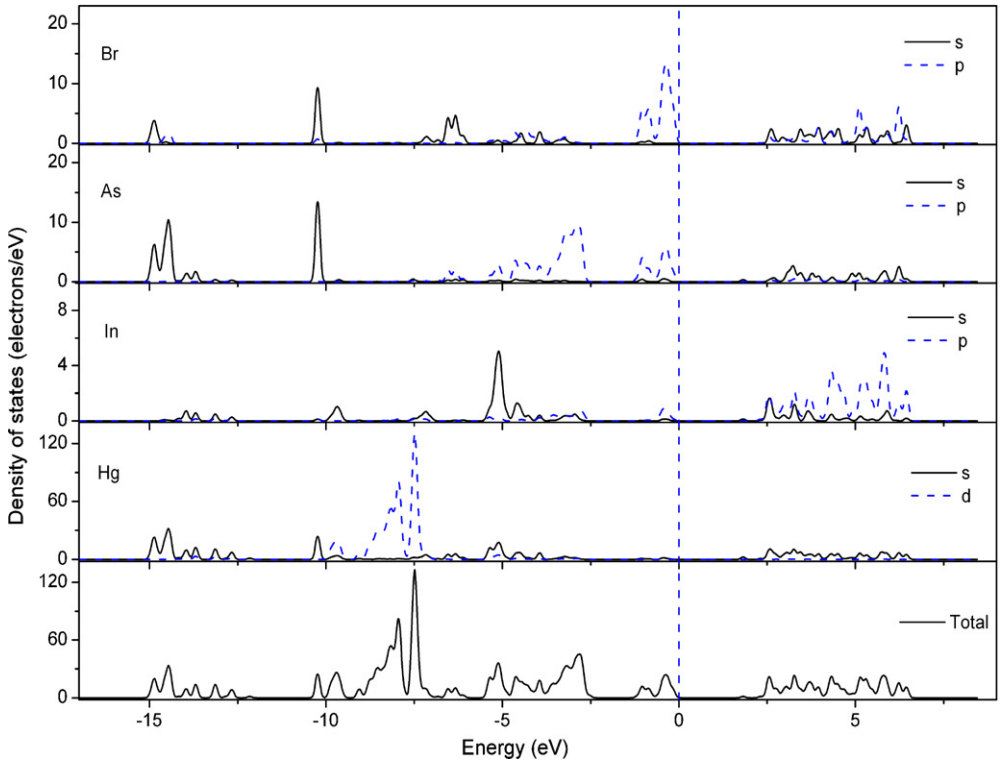

Fig. 4. The total and partial density of states for **1** (the Femi level is set at 0 eV).

from 3.81 to 3.87 Å, which are much longer than the normal Hg–Br covalent bond distance (2.64 Å) and shorter than the sum of van de Waals radii of Hg and Br atoms. Thus, the host–guest supramolecular interactions fix the guest anions to their specific position so that no position or rotational disorder is observed for them, which is also found in the literatures [24–28,32–35].

The diffuse reflectance spectrum of **1** reveals the presence of an optical gap of 1.71 eV (Fig. 2), which suggests that the present compound is semiconductor and consistent with its color. The IR spectrum of **1** shows no obvious absorption in the range of 4000–400 cm^{-1} (Fig. S1), which supports the idea that the compound may be potentially used as window materials for laser delivery media and infrared transmitting for optical fiber applications in telecommunication [49,50].

The calculated band structure of **1** along high symmetry points of the first Brillouin zone is plotted in Fig. 3, where the labeled *k*-points are present as G (0.0, 0.0, 0.0), A (0.0, 0.0, 0.5), H (−0.333, 0.667, 0.5), K (−0.333, 0.667, 0.0), M (0.0, 0.5, 0.0), and L (0.0, 0.5, 0.5). It is found that the top of valence bands (VBs) has small dispersion, whereas the bottom of conduction bands (CBs) has big dispersion. The lowest energy (1.58 eV) of CBs is localized at G point, while the highest energy (0.00 eV) of VBs is localized at K point. According to our calculations, the solid-state compound **1** thus shows a semiconducting character with an indirect band gap of 1.58 eV, which is comparable with the experimental value (1.71 eV). The bands can be assigned according to total and partial densities of states (DOS), as plotted in Fig. 4. The Hg-5d, Br-4 s and As-4s states, mixing with small Hg-6s and In-5s states, create the VBs localized between −17.5 and −5.0 eV. The VBs between −5.0 eV and the Fermi level (0.0 eV) are mostly formed by Br-4p and As-4p states mixing with a small amount of the Hg-6s and In-5s states, while the CBs between 1.5 and 8.0 eV are almost contribution from Hg-6s and In-5p states hybridized with a small amount of In-5s, Br-4s, Br-4p and As-4s states. Accordingly, it can be considered that the optical absorption of **1** is mainly ascribed to the charge transitions from Br-4p and As-4p states to Hg-6s and In-5p states.

Semiempirical population analysis allows for a more quantitative bond analysis. The calculated bond orders of the In–Br, Hg–As and Hg–Br are from −0.09 to 0.05, 0.56 to 0.81, and −0.39 to −0.16 e in a unit cell of **1** (pure covalent single bond order is generally 1.0 e), respectively. Accordingly, it indicates that the Hg–As bond is mainly covalent character, while the In–Br bond is mainly ionic character. And there are only weak interactions between Hg and Br, which are in good agreement with the crystal structure of **1**.

4. Conclusion

In the present work, a new quaternary supramolecular compound $[Hg_4As_2](InBr_{3.5}As_{0.5})$ has been synthesized and characterized, which exhibits a new type of open-framework with tridymite topology. And the anionic chains are embedded in the channels of the host open-framework. The diffuse reflectance spectrum of **1** reveals the presence of an optical gap of 1.71 eV, and the IR spectrum of **1** shows no obvious absorption in the range of 4000–400 cm^{-1}. The calculations of the electronic band structure along with density of states (DOS) indicate that the present compound is a semiconductor with an indirect band gap, and that the optical absorption is mainly originated from the charge transitions from Br-4p and As-4p states to Hg-6s and In-5p states.

Acknowledgements

We gratefully acknowledge the financial support of the NSF of China (20801026), the NSF of Jiangxi Province (2008GQC0036), the Aviation Science Foundation of China (2008ZF56012), Foundation of State Key Laboratory of Structural Chemistry (20100015), and Open Fund of the Key Laboratory of Nondestructive Testing, Ministry of Education, Nanchang Hangkong University (ZD200929007).

Appendix A. Supplementary data

The molecular structure of **1** and IR spectral figure are available. Further details of the crystal structure investigation(s) can be obtained from the Fachinformationszentrum Karlsruhe, 76344 Eggenstein-Leopoldshafen, Germany, (fax: +49 7247 808 666; e-mail: crysdata@fiz-karlsruhe.de) on quoting the depository number CSD-421382.

Supplementary data associated with this article can be found, in the online version, at doi:10.1016/j.jallcom.2010.09.035.

References

[1] M.E. Davis, Nature 417 (2002) 813–821.
[2] P. Feng, X. Bu, N. Zheng, Acc. Chem. Res. 38 (2005) 293–303.
[3] A. Corma, M.J. Díaz-Cabañ, J.L. Jordá, C. Martínez, M. Moliner, Nature 443 (2006) 842–845.
[4] S. Dehnen, M. Melullis, Coord. Chem. Rev. 251 (2007) 1259–1280.
[5] J. Yu, R. Xu, J. Mater. Chem. 18 (2008) 4021–4030.
[6] D.M. Shin, I.S. Lee, Y.K. Chung, Cryst. Growth Des. 6 (2006) 1059–1061.
[7] C. Qin, X. Wang, L. Carlucci, M. Tong, E. Wang, C. Hu, L. Xu, Chem. Commun. (2004) 1876–1877.
[8] J.B. Parise, Inorg. Chem. 24 (1985) 4312–4316.
[9] W. Schnick, J. Luecke, Angew. Chem. 104 (1992) 208–209.
[10] M. Roca, M.D. Marcos, P. Amoros, A. Beltran-Porter, A.J. Edwards, D. Beltran-Porter, Inorg. Chem. 35 (1996) 5613–5621.
[11] C.I. Bows, G.A. Ozin, Adv. Mater. 8 (1996) 131–135.
[12] W. Schnick, Stud. Surf. Sci. Catal. 84 (1994) 2221–2224.
[13] S.I. Zones, R.J. Darton, R. Morris, S.J. Hwang, J. Phys. Chem. B 109 (2005) 652–661.
[14] L.A. Villaescusa, P.A. Barrett, M.A. Camblor, Angew. Chem. Int. Ed. 38 (1999) 1997–2000.
[15] R.L. Bedard, S.T. Wilson, L.D. Vail, J.M. Bennett, E.M. Flanigen, Stud. Surf. Sci. Catal. 49 (1989) 375–377.
[16] J.B. Parise, J. Chem. Soc., Chem. Commun. (1990) 1553–1554.
[17] C.L. Cahill, Y. Ko, J.B. Parise, Chem. Mater. 10 (1998) 19–21.
[18] O.S. Oleneva, A.V. Olenev, E.V. Dikarev, A.V. Shevelkov, Eur. J. Inorg. Chem. (2004) 4006–4010.
[19] A.V. Olenev, O.S. Oleneva, M. Lindsjö, L.A. Kloo, A.V. Shevelkov, Chem. Eur. J. (2003) 3201–3208.
[20] A.V. Olenev, A.V. Shevelkov, Angew. Chem. Int. Ed. 40 (2001) 2353–2354.
[21] J.-P. Zou, G.-C. Guo, W.-T. Chen, X. Liu, M.-L. Fu, Z.-J. Zhang, J.-S. Huang, Inorg. Chem. 45 (2006) 6365–6369.
[22] A.V. Olenev, A.I. Baranov, A.V. Shevelkov, B.A. Popovkin, Eur. J. Inorg. Chem. (2000) 265–270.
[23] J.-P. Zou, Y. Li, Z.-J. Zhang, G.-C. Guo, X. Liu, M.-S. Wang, L.-Z. Cai, Y.-B. Lu, J.-S. Huang, Inorg. Chem. 46 (2007) 7321–7325.
[24] H. Puff, M. Grönke, B. Kilger, P. Möltgen, Z. Anorg. Allg. Chem. 518 (1984) 120–124.
[25] J. Beck, S. Hedderich, U. Neisel, J. Solid State Chem. 154 (2000) 350–355.
[26] A.V. Shevelkov, M.M. Shatruk, Russ. Chem. Bull. Int. Ed 50 (2001) 337–362.
[27] J.-P. Zou, S.-P. Guo, X.-M. Jiang, G.-N. Liu, G.-C. Guo, J.-S. Huang, Solid State Sci. 11 (2009) 1717–1721.
[28] J.-P. Zou, Y. Li, M.-L. Fu, G.-C. Guo, G. Xu, X.-H. Liu, W.-W. Zhou, J.-S. Huang, Eur. J. Inorg. Chem. (2007) 977–984.
[29] L. Nijssen, W.N. Lipscomb, Acta Crystallogr. 7 (1954) 103–106.
[30] W.R. dorff, K. Brodersen, Z. Anorg. Allg. Chem. 274 (1953) 323–340.
[31] R. Airoldi, G. Magnano, Rass. Chim. 5 (1967) 181–189.
[32] A.V. Shevelkov, M.Y. Mustyakimov, E.V. Dikarev, B.A. Popvkin, J. Chem. Soc., Dalton Trans. 1 (1996) 147–148.
[33] A.V. Olenev, A.V. Shevelkov, B.A. Popovkin, Zh. Neorgan. Khim. 44 (1999) 1853–1856.
[34] A.V. Olenev, A.V. Shevelkov, B.A. Popovkin, Zh. Neorgan. Khim. 44 (1999) 1814–1816.
[35] J.-P. Zou, D.-S. Wu, S.-P. Huang, J. Zhu, G.-C. Guo, J.-S. Huang, J. Solid State Chem. 180 (2007) 805–811.
[36] W.W. Wendlandt, H.G. Hecht, Reflectance Spectroscopy, Interscience Publishers, New York, 1966.
[37] G. Kortüm, Reflectance Spectroscopy, Springer-Verlag, New York, 1969.
[38] Siemens SHELXTL™ Version 5 Reference Manual, Siemens Energy & Automation Inc., Madison, Wisconsin, USA, 1994.
[39] M. Segall, P. Linda, M. Probert, C. Pickard, P. Hasnip, S. Clark, M. Payne, Materials Studio CASTEP Version 2.2, 2002.
[40] D.R. Hamann, M. Schluter, C. Chiang, Phys. Rev. Lett. 43 (1979) 1494–1497.
[41] M. Segall, P. Linda, M. Probert, C. Pickard, P. Hasnip, S. Clark, M. Payne, J. Phys.: Condens. Matter 14 (2002) 2717–2744.
[42] J.P. Perdew, K. Burke, M. Ernzerhof, Phys. Rev. Lett. 77 (1996) 3865–3867.

[43] S.-P. Huang, W.-D. Cheng, D.-S. Wu, X.-D. Li, Y.-Z. Lan, F.-F. Li, J. Shen, H. Zhang, Y.-J. Gong, J. Appl. Phys. 99 (2006) 0135161–0135164.
[44] A.V. Shevelkov, E.V. Dikarev, B.A. Popvkn, J. Solid State Chem. 126 (1996) 324–327.
[45] A.V. Shevelkov, E.V. Dikarev, B.A. Popvkn, Zh. Neorgan. Khim. 40 (1995) 1496–1501.
[46] T. Staffel, Z. Anorg. Allg. Chem. 552 (1987) 113–122.
[47] H. Baernighausen, Z. Anorg. Allg. Chem. 186 (1989) 16–18.
[48] T. Staffel, G. Meyer, Z. Anorg. Allg. Chem. 582 (1990) 128–130.
[49] J.A. Harrington, Infrared Fibers and Their Applications, SPIE Press, Bellingham, WA, 2004.
[50] D. Marchese, M. De Sario, A. Jha, A.K. Kar, E.C. Smith, J. Opt. Soc. Am. B 15 (1998) 2361–2370.